

Abel Cavalcante Lima Filho

abel@les.ufpb.br
Federal University of Paraíba
Mechanical Engineering Department
58051-900 João Pessoa, PB, Brazil.

Francisco Antônio Belo

belo@les.ufpb.br
Federal University of Paraíba
Electrical Engineering Department
58051-900 João Pessoa, PB, Brazil

Jerry Lee Alves dos Santos

jerry@les.ufpb.br
Federal University of Paraíba
Computer Science Department
58051-900 João Pessoa, PB, Brazil

Eudisley Gomes dos Anjos

eudis@dei.uc.pt
University of Coimbra
Department of informatics Engineering
3030-290 Coimbra, Portugal

Experimental and Theoretical Study of a Telemetric Dynamic Torque Meter

This paper presents the development of a dynamic torque meter to be applied to rotating shafts using electronic transduction, strain gage, telemetry and LabView Graphic programming. A mathematical model was developed. The electronic transduction signal is transmitted by digital modulation from a remote transduction unit fixed to a shaft to a base station, sending the signal to a PC, by means of a VI (Virtual Instrument) developed in LabView. It can also be delivered to other units besides the PC. The use of digital modulation to transmit the radiofrequency signal, replacing conventional couplings, allows communication with a high signal/noise ratio. A clamp acts as sealant, protecting it from the environment and making it easier to install. The prototype can be used at situation that it is impossible to use flanges or sockets (the most of the industrial applications) and it is installed directly on the surface of the shaft. The use of superbatteries allows the remote unit to remain independent of a feed for several days, with long periods between maintenance. After thousands of experimental essays, the theoretical model seems to confirm the proposed idea. The system presented has a potential for high precision, low cost, long work life and easy maintenance.

Keywords: dynamic torque meter, telemetry, strain gage, electronic transduction and transduction by LabView

Introduction

The quality of a product manufactured in an industrial process is intrinsically linked to appropriate monitoring and to accurate measurement of the magnitudes that influence its performance. Instruments are needed to ensure efficiency and quality, and to provide safety for all of the equipment and personnel involved in the process (Preobrazhensky, 1980). In this context, torque is one of the most important characteristics of the parameters for machines used in production. Currently used torque meters do not fulfill the requirements, and a short term solution must be found to develop torque transducers that will have a broad range of action, high definition, low depreciation over time, and that are easy to install (Meng and Liu, 2006).

This study proposes to create a dynamic torque meter that will fulfill the abovementioned requirements, at low cost and with long intervals between maintenance.

Currently, there are very accurate instruments, depending on what they are used for, to obtain static torque, but there are still great challenges when one wishes to measure dynamic torque. Most energy conversion or transfer processes use rotating mechanical devices, and there is great interest in obtaining an adequate measuring system, which has led to several studies throughout history. Since companies in this industry have a financial interest in the issue, the final approach to the instrument is sealed to prevent the technical analysis of its constituent parts, keeping this product an industrial secret. This is reflected by the absence of technical publications regarding the architecture of these devices (Brito, 1994).

It is essential to understand the type of torque to be measured, as well as the different types of torque meters available, in order to choose the method that will fulfill the project requirements at a

lower cost. Moreover, according to the criteria used to select the appropriate dynamic torque meters, the range of action should observe, together with accuracy, maximum rotation frequency, resistance to environmental conditions, overload capacity and transduction circuit which can minimize noise during the signal transmission and saturation (Norton, 1969).

The first dynamic torque meter known was the Prony torque meter, invented by Gaspar de Prony (1755-1839). It used the absorption method, which consists of absorbing the mechanical energy present in the rotating shaft by braking (Holman, 1984).

In 1877 Sir William Froude invented the torque meter, which became known as the water brake, consisting of a unit that is placed in a sequence with the shaft of the machine being tested, formed basically by a rotor covered by a housing full of water (or some other fluid), a metal arm and scales. Using an absorption mechanism, the rotor supplies the housing, through the free fluid inside it, with a torque that can be read by the scales connected to it by a metal arm (Enciclopedia Britannica, 1986).

Presently, the torque meters that use an ERSG (electrical resistance strain gage) are most popular to obtain torque in rotating shafts. The electrical resistance strain gage is the most widely used sensor to read strain and its derivatives thanks to characteristics such as calibration stability, small variation caused by environmental factors, accuracy, dynamic response compatible with frequencies over 100 kHz allowing remote operation, with a good response to temperature variations, low cost, widespread use, easy installation, easy operation and a linear response to a wide range of uses (Dally, Riley and McConnell, 1993).

Currently, the study of dynamic torque meters focuses mainly on allowing data transfer, which will minimize noise caused by rotation, with a high resolution, resistant to environmental factors and with the longest possible work life.

The slip rings method is commonly used to feed and transfer data in dynamic torque meters. It consists basically of a set of guide rings coupled to the shaft, and a series of stationary brushes,

which are in contact with the rings, capturing information and feeding the circuit.

Slip ring abrasion is a great problem in this method because it reduces instrument accuracy (Cheong et al., 1999). Due to the noise caused by friction between the brush and rings in applications above 10,000 rpm, great care must be taken to avoid problems caused by heating and vibration, although it is operated successfully at up to 100,000 rpm approximately (Doebelin, 1990).

The method using rotating transformers was developed to avoid problems caused by the slip rings. By eliminating the brushes and rings, long term wear and tear of the material is avoided, besides eliminating the parasite torques from friction. However, the need for bearings and the fragility of the transformer core do not increase the maximum rotation speed of the shaft significantly, and the system also becomes susceptible to noises and errors caused by the alignment between the primary and secondary coils of the transformer. A specialized signal conditioner is required to produce a reliable signal when data are acquired, making the system more expensive than the ensemble of slip rings.

The infrared method of signal transmission uses a rotating transformer to supply energy required by the strain gage bridge. An A/D converter in the shaft transmits its output signal through infrared light from the rotating shaft to the stationary diodes. Since this method uses wireless technology, it also prevents the undesirable phenomena caused by friction and wear of the connectors, besides making it possible to have a very high signal/noise ratio due to digital transmission of the information, however presents, most of the time, low immunity under abrasive environments and a high cost compared with the other methods.

Besides the methods described using ERSO, the method to obtain torque by reading the torsion angle has been intensively studied. An important parameter of this type of instrument is to choose a shaft which will allow good resolution and have a high frequency of resonance. However, the need to develop robust encoding that will achieve good sensitivity to small torsion angles is still a great challenge, since the maximum torsion angle for the sensitive part is in the range of 0.25° for each meter of shaft length (Cheong, 1999).

In recent years, several studies were performed to obtain torque using fiber Bragg grating (FBG) sensors to replace ERSO (Tian, Wang and Kruger, 2000, 2001, 2004) and a magnetostrictive sensor that changes shape according to the magnetic field to which it is submitted (Olabi, 2006). However, both present complex implementation and restricted applications.

The radiofrequency instrumentation method has become quite popular, especially since studies were performed on electronic transduction, allowing the transmission of very high signal/noise ratio signals. An induction power supply is used to feed the circuit and to transmit signals (Sensotec, 2007). This source contains an oscillator that works at high frequencies, whose signal is fed by current amplifiers. These amplifiers drive a resonant transformer/capacitor circuit through the stationary antenna. The oscillator is coupled to the circular antenna fixed to the rotating shaft which transmits the signal in radiofrequency to the stationary antenna. This signal is filtered in the oscillator frequency range, and allows reading the signal by means of a microcontroller and a display or a conventional PC, for instance.

This method, as well as the infrared, eliminates the noise caused by the system of rotating transformers and slip rings, besides allowing simple, cheaper installation, compared to the infrared. However, its application is limited due to the inconvenience of changing batteries, positioning the induction power source and, in some cases, to the noise caused by vibrations of the axis.

This paper presents a Telemetric Dynamic Torque Meter based at strain gage sensor applied to shafts, electronic transduction,

telemetry and LabView Graphic programming. The system proposed does not present the problem above cited of the other instruments, or it does very lower.

Nomenclature

d	= diameter, m
ERSO	= electrical resistance strain gage
f_{max}	= maximum frequency, Hz
G	= transverse elasticity modulus, Pa
L	= length of strain gage grid, m
L	= length of metallic arm, m
BSTM	= base station transceiver module
FNTM	= field node transceiver module
P	= weight, N
R	= electrical resistance, $ohms$
S	= sensitivity, dimensionless.
T	= torque in solid shaft, Nm
T_p	= peak torque, Nm
V	= voltage, V
VP	= sound propagation velocity on the shaft, m/s
VS	= output voltage from the transduction electronics, V
$V_{off-set}$	= residual voltage, V

Greek Symbols

ΔV	= voltage variation, V
ε	= strain, dimensionless
λ	= wavelength, m

System Description

Figure 1 illustrates a basic system for ERSO torque meters. On the rotating shaft, the ERSO, present in a wheatstone bridge, reads the torque and the corresponding analog signal is sent to the signal pre-conditioner, where the power and data are transferred with a (stationary) conditioner. Then, the signal is made available to read the torque.

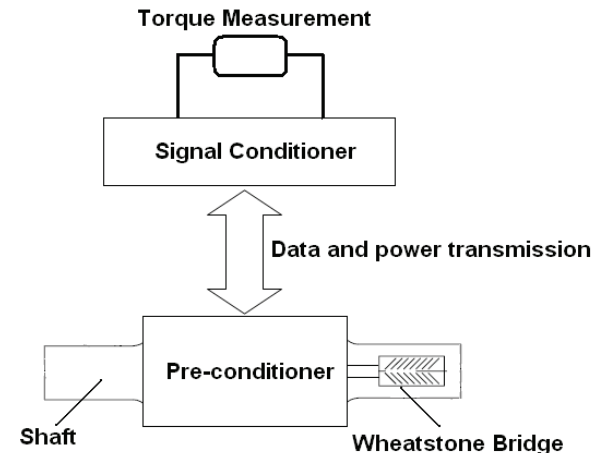


Figure 1. Schematic of torque acquisition by ERSO.

The system proposed by this study works according to the schematic shown in Fig. 2. The signal from shaft deformation, picked up by the strain gage, is processed and amplified by the electronic transduction circuit and sent to the FNTM (field node transceiver module). In the FNTM, the analog signal is converted into digital by a microcontroller and transmitted to a transceiver chip which modulates the signal in phase (phase shift keying – PSK) and excites the full duplex antenna, radiating the signal by

radiofrequency. In the base station transceiver module BSTM (base station transceiver module) the RF signal picked up by the helical antenna is filtered through the transceiver chip, filtered (narrow-band filter), demodulated, amplified and made available for reading. The reading can be performed using a PC (embedded or conventional), or made available by the 4 to 20 mA pattern (high immunity to noise) and/or MODBUS protocol in industrial applications.

Figure 3 illustrates the UML diagram showing the adaptation sequence for acquisition and laboratory tests through a LabView program. The system activates the RF module of the base, which sends a signal to activate the remote module located at the reducer shaft exit. The data are obtained by remote sensor, converted to digital and sent to the base sensor which passes them on to the system. Torque is then calculated and shown on the screen.

An advantage of the system shown is that it is unnecessary to use flanges or sockets like the commercial dynamic torque meters. The installation is done directly on the surface of the shaft involved and calibrated right there, and it can thus be used for many types of application.

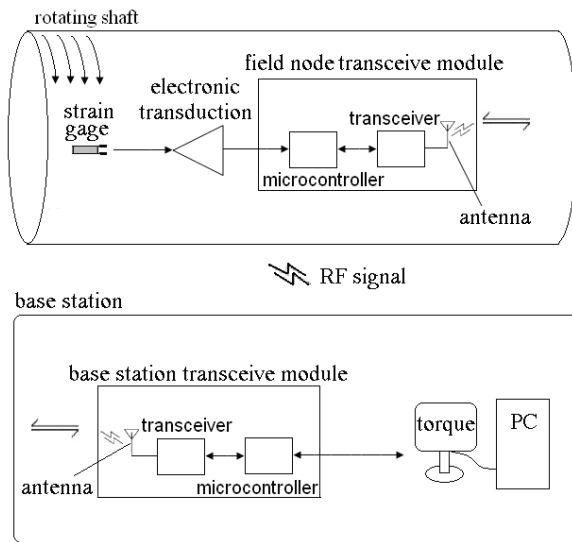


Figure 2. Schematic of the radiofrequency instrumentation system proposed by this study.

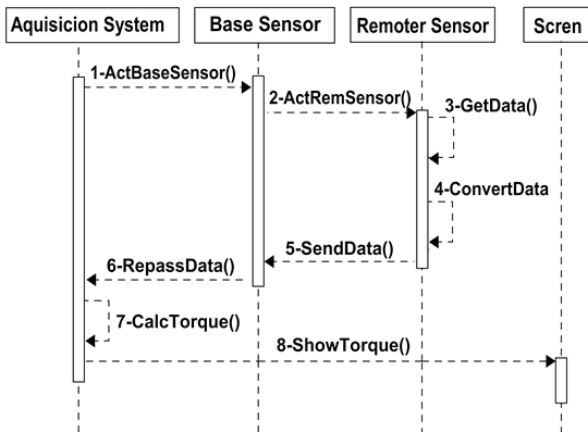


Figure 3. Sequence diagram (torque acquisition in the laboratory).

System Design and Development

System data acquisition begins with a deformation on the shaft read by the strain gage. The operational principle of a strain gage is the property that allows it to vary its resistance when the surface with which it is in contact suffers some deformation. This change obeys Eq. (1).

$$\frac{dR}{R} = \epsilon S \tag{1}$$

where dR is the little electrical resistance variation; R is the electrical resistance, Ω ; ϵ is the strain; and S is the sensitivity of strain gage.

Strain gage sensitivity depends on the material from which it is made. It usually ranges from 2 to 4 for many metal alloys. When using strain gages, it is necessary to observe which metal one wishes to deform, and then choose a strain gage with an alloy that responds to a temperature similar to that of the metal involved, in order to minimize errors. In this study, a strain gage was used with a standard resistance of 350 ohms and temperature compensation compatible with the shaft material.

It is the mechanics of solids that a pure shear undergoes an axis of circular cross section which provides tensions normal values and equal angles of the 45° positive and negative, in relation to the length of the shaft, and that the strain gages are sensitive only to the normal tensions in relation to the length of their metal wires. Thus, the shear stress can be measured by positioning strain gages at angles of $\pm 45^\circ$ relative to the length of the shaft. Therefore, for a shaft with a solid cross-section with a d diameter, torque can be determined using Eq. (2).

$$T = \frac{\pi G d^3 \epsilon}{8} \tag{2}$$

where T is the torque submitted to the shaft, Nm; G is the transverse elasticity modulus of the material, Mpa; and D is the diameter, m

From Eqs. (1) and (2), a relation can be obtained between torque and the variation of resistance in the strain gage dR , as shown in Eq. (3):

$$T = \frac{\pi G d^3}{8S} \frac{dR}{R} \tag{3}$$

In order to make it easier to process the signal obtained by the strain gage, resistance is converted to voltage through the Wheatstone bridge in the transduction electronics circuit.

An alternating current signal feeding a Wheatstone bridge and a synchronous demodulator are presented by "Analog Devices" for solution with strain gage circuits (Gerstenhaber and Lee, 2004). The Research Group for Instrumentation and Control in a Study of Energy and the Environment (GPICEEMA – Grupo de Pesquisa em Instrumentação e Controle em Estudo de Energia e Meio Ambiente) developed a circuit based on a different proposal from that of Analog Devices, with a similar performance, less power consumed, greater integration, lower cost and use of components that are easily available on the market. The circuit, which was also widely tested in thermoresistive transduction, presented simulations for a temperature variation of 50°C , with an excellent performance, and an error of 0.05% of full scale. Figure 4 shows a simplified diagram of this circuit.

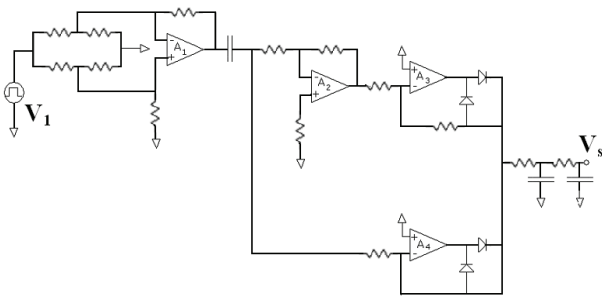


Figure 4. Electronic transduction circuit proposed by this article.

Processing is done by a transceiver using the ZigBee Protocol (IEEE 802.15.4) of radiofrequency communication. ZigBee was chosen due to its viability for on-board applications, which require low energy consumption. The module used is XBee from MaxStream, and it is processed by a microcontroller and a transceiver which transmit the data at a rate of up to 125 kb/s at a frequency of 2.4 GHz, and it reaches up to 100 m. This module has a 10-bit resolution A/D converter, it has 8 analog entry channels and in-phase modulation (PSK) for digital transmission of information. This module can be configured using X-CTU software, which allows writing and modifying firmware as required by the application.

Software was used to program the Xbee to send a reading through a package during a 1 ms sampling period, and the analogical input was enabled. An interface board was made for the Xbee to ensure reference voltage and a 3V feed using two LT1761ES5-3 regulators, according to the circuit in Fig. 5. The board layout and the capacitors used were designed to minimize the noise, which is part of the voltage regulation process.

The remote unit set (strain gage – transduction electronics – FNTM) is comprised of sensitive integrated circuits technology. Due to the sensitivity to the weather and the rotation of the reducer shaft, GPICEEMA developed a clamp with a flexible fiberglass sealant for protection and fixation of this circuit, designed in such a way that its measurement acquisition will not be influenced (Author, 2007). The clamp shown in Fig. 6, which is the subject of a patent of invention, is coupled to the shaft, sealed and the moisture is removed, and all the components of the remote unit are inserted in it.

Some Limits of Use

In designing the system, it is very important to verify the limit or range of use of the components regarding the magnitude at which work is done. For the telemetric system proposed by this study, it is necessary to size the devices appropriately, maximizing their work life and minimizing the acquisition errors.

Since the strain gage is to be used to measure torsion in a shaft submitted to angular acceleration, a few precautions must be taken about its dynamic behavior. It is necessary to establish a maximum frequency of use of the strain gage so that the response time is compatible with shaft rotation. Therefore, the length of the strain gage grid l must be much less than the wave length λ (wavelength) of the mechanical vibrations of the shaft. In order to ensure that the strain gage will operate perfectly, $l \leq 0.1\lambda$ (Antunes, 2003) is adopted.

It is known that the maximum frequency of use of a strain gage, adopting the criterion of $l = 0.1\lambda$, is given by:

$$f_{max} = \frac{V_P}{10l}$$

where f_{max} is the maximum frequency, Hz; V_P is the velocity of sound propagation at the shaft, m/s; and l is the length of strain gage grid, mm.

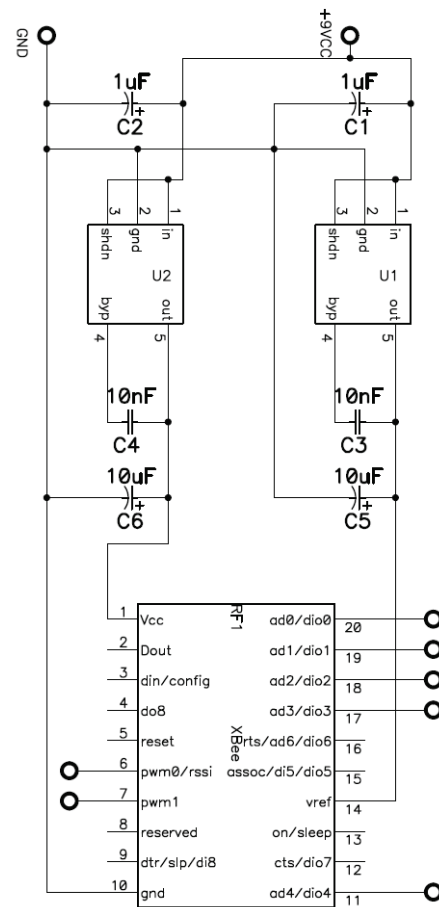


Figure 5. Printed circuit to regulate voltage in the remote unit.

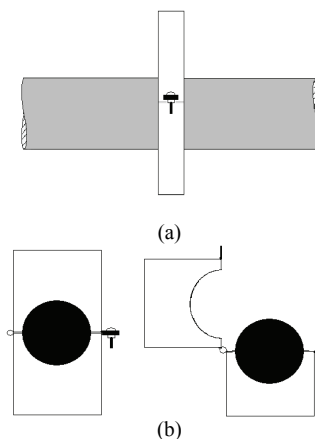


Figure 6. Clamp and flexible sealant for the remote unit set. a) Front view, b) Side view.

In the case of carbon steel SAE/ABNT 1045 where $V = 5950$ m/s and using a strain gage with a grid size $l = 6.35$ mm, $f_{max} = 94$ kHz is obtained. Therefore, the time of action of the strain gage is sufficiently compatible with the dynamic response for most applications.

Another point that should be looked at is the maximum torque that can be borne by the strain gage. The strain gage used in this study allows at most 10^6 cycles of $1500 \mu\epsilon$, and thus, for the strain

gage to have a theoretically infinitely long work life it is necessary for it to work with deformations below this value. Using the solid mechanics theory, it is calculated that this strain gage can work with torques of up to 2,312,766 in.lb or 261.3 kN.m.

Another limit that must be taken into account is the value which will be caused by electronic transduction saturation. As seen in the previous section, the circuit was sized for a variation of up to 2Ω at each bridge strain gage. Based on Eq. (3) it is calculated that for $R = 350 \Omega$, $S = 2.08$ and $\varepsilon = 1500 \mu\epsilon$, $dR = 1.092$ ohms is obtained. Therefore, it is concluded that the circuit will never be saturated, since the maximum deformation of the strain gage is well below the value subject to electronic saturation.

Due to the low consumption of the electronic components present in the remote unit, it is estimated that the total voltage drained is on the order of 50 mA. Considering that the super battery consumption is 19 A.h, the time for the battery to begin to discharge would be $20 \text{ A.h} / 50 \text{ mA} = 400 \text{ h}$ (around 17 days). In order to monitor torque in a mechanical pumping unit used to extract oil, each acquisition will last ten seconds at 15-minute intervals. In this case the system can be run autonomously for approximately 4 years.

Analysis of the Results

The commercially available dynamic torque meters are calibrated by static torque (Fujii et al., 1999) and the calibration of torque as a whole (with all the mechanical variables found) is not practicable according to the state of the art, and, therefore, the torque meter must be calibrated before applying it directly to the structure and estimating future dynamic behavior under the working conditions (Wegener and Andrae, 2006). This torque meter was designed to be calibrated directly at the site where it is applied, but the bench in Fig. 7 was made for precision and feasibility studies of the method employed.

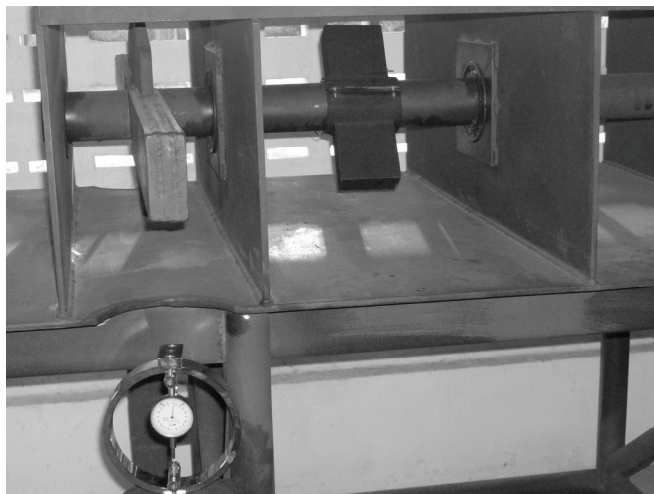


Figure 7. Static torque bench to study the method.

The bench in Fig. 7 has a shaft with a circular steel section, 80 mm in diameter and 1.85 m long, fixed by soldering at one end. Almost at the tip of the other end, a stiff stem was soldered, transverse to the prototype shaft. In order to the torque applied to the shaft to have pure shear stress, or negligible normal stress, the shaft was coupled to a bearing formed by three sheets soldered to the table in such a way that it will not influence torsion (Fig. 7).

After the strain gauge was installed, its terminals were interlinked with the electronic transduction circuit and the latter to the FNTM. The ensemble was fitted in the brace, whose size is compatible with the circuit, and then it was coupled to the shaft.

More or less 30 meters from the simulation bench, the BSTM was connected to the PC through a USB port.

For the program to calculate torque through the signal emitted, a torque curve must be generated considering the voltage at the transducer terminals. When this curve is inserted into the program, it will allow the torque to be calculated and shown on the screen, i.e., the program receives voltage and supplies torque.

When the experiment was performed, the transducer was arranged to supply the transceiver module with voltage according to Eq. (4).

$$dR = 0.5422 * \Delta V \tag{4}$$

where ΔV is the voltage variation in transduction electronics circuit due dR . And it is given for:

$$\Delta V = V_S - V_{off-set}$$

where V_S is output voltage from the transduction electronics and $V_{off-set}$ is the residual voltage present in the absence of torque (off-set voltage).

Relating this to Eq. (3) and Eq. (4) we obtain torque as a function of the output voltage obtained from the transduction circuit.

$$T = \frac{\pi G d^3}{14.75 S R} \Delta V \tag{5}$$

Thus, for each deformation read on the surface of the strain gage, we have a way to calculate its equivalent torque.

Considering data $G = 80 \text{ GPa}$ (ABNT/SAE1045 steel); $d = 0.079 \text{ m}$; $S = 2.08$ and $R = 350$; and substituting them in Eq. (5) the following is obtained:

$$T = 11536.29 * \Delta V \tag{6}$$

When the program is executed, the value of torque for a given voltage at the exit from the transducer, originating from a deformation, can be seen on the screen. Figure 8 illustrates the basic components of the system and how they are disposed when reading torque in real time.

In order to obtain torque using the dynamometer, the following were positioned (from bottom up) on a support base on the bench: the hydraulic jack, the dynamometric ring and a small prism, in contact with the metal vane, to demarcate the line where force is being exerted in relation to the shaft. Once the value of the force applied is known, torque is obtained automatically multiplying force by the distance between the point of support and the shaft (Fig. 9). Then:

$$T = F \times L$$

where T is the torque applied to the shaft; F is the force applied to the metal arm; and L is the distance between the shaft and the point where the force is being applied.

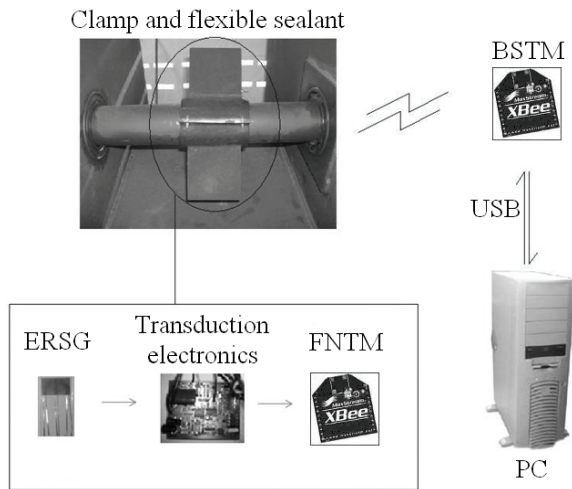


Figure 8. Basic components of the system to acquire torque in real time at the laboratory.

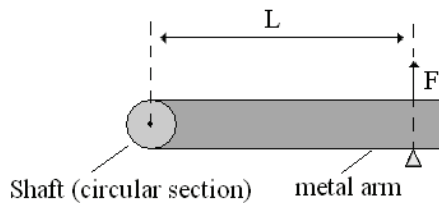


Figure 9. Calculating static torque.

After calibrating the dynamometric ring, different torque values were applied to the metal arm soldered to the shaft where the data obtained by the dynamometer and those obtained on the computer screen using the LabView program were recorded (Fig. 10).

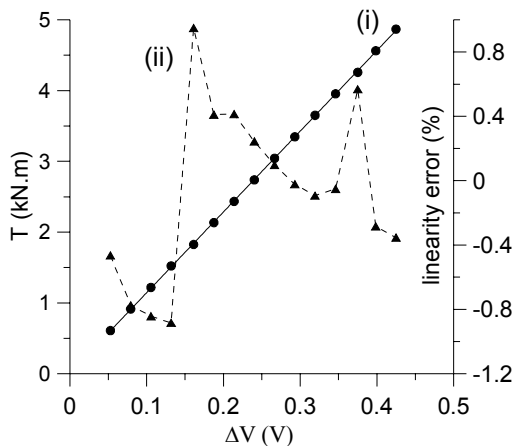


Figure 10. Experimental results: (i) Regression curve for static torque calibration; (ii) the linearity error with respect to the best-fit line.

Table 1 relates the torque obtained by a reference instrument (regression curve of Fig. 10) and the torque calculated by Eq. (6) from the torque meter created by this study (LabView), using the transmitted voltage variation from the remote unit.

Using the data in Fig. 10 and Table 1 respectively we reach instrument uncertainty of 0.54% (linearity error) for static torque and a mean error of method of 0.20% (based on Eq. (6)).

Table 1. Reading the torque using the dynamic torque meter created at a static bench.

ΔV (V)	Reference Torque (kNm)	Calculated Torque (kNm)	Error
0.052734	0.606066	0.603623	-0.40%
0.079102	0.906803	0.905446	-0.15%
0.105469	1.207528	1.207258	-0.02%
0.131836	1.508253	1.509069	0.05%
0.161133	1.842396	1.844419	0.11%
0.187500	2.143121	2.146231	0.15%
0.213837	2.443504	2.447699	0.17%
0.240234	2.744571	2.749854	0.19%
0.266602	3.045307	3.051677	0.21%
0.292969	3.346032	3.353488	0.22%
0.319336	3.646757	3.655300	0.23%
0.346103	3.952044	3.961690	0.24%
0.375000	4.281625	4.292461	0.25%
0.398437	4.548933	4.560734	0.26%
0.424805	4.849669	4.862557	0.27%

For the first acquisitions of dynamic torque, the dynamic torque I bench of Fig. 11 was made, which consists of a 760 W motor, with a rotation velocity of 1680 rpm coupled to a gear reducer which supplies an output rotation of 86 rpm. At the extremity of the reducer exit shaft an aluminum pulley was soldered, where a belt will connect it to a metal arm. Applying force downwards on the metal arm, the pulley is broken, and consequently a torque is applied to the reducer shaft.

Similarly to the schematic of the previous section, the strain gage was installed on the shaft and then the brace containing the transduction circuit and the FNTM was coupled.

The same procedure as the static torque bench was performed to acquire the data via PC, through Eq. (3). Now, however, the following data were used: $G = 80$ GPa (ABNT/SAE1045 steel); $d = 0.03$ m; $S = 2.08$; $R = 350$; and $dR = 0.872 * \Delta V$, what results:

$$T = 1016 * \Delta V$$

The motor was switched on and the experiment was performed for different torque values, whose curves can be seen in Fig. 12.

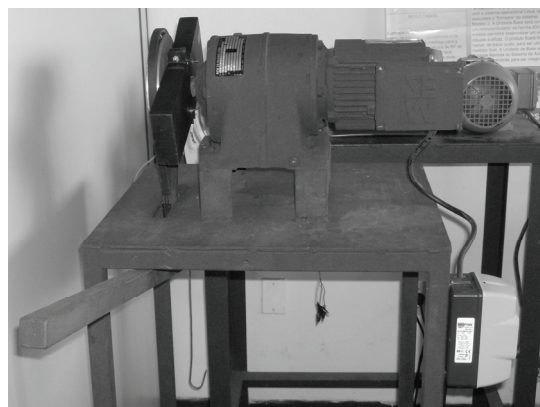


Figure 11. Dynamic torque I bench.

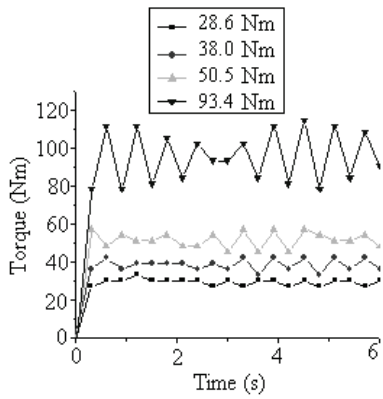


Figure 12. Torque (Nm) x time (s) graphs.

No loss of connection occurred during the experiment, and it is estimated that the noise (louder for higher torque value) occurred due to an imperfection at the output shaft of the reducer of the bench used, so that a translation movement occurs, not only pulley rotation. Figure 13 shows linear regression for the curves in Fig. 12. Linearity is noted in the mean of readings, which proves a possible translation movement of the shaft.

The bench in Fig. 14 was made to look at the data acquisition capacity of the system for dynamic behavior, and to confirm the feasibility of applying it.

The bench was made to simulate the torque at the exit from the reducer of a mechanical pumping unit, where shaft velocity is relatively slow. It consists of a 550 W motor, with a rotation speed of 1680 rpm, coupled to a back gear which supplies an output rotation of around 17 rpm. At the extremity of the reducer exit shaft, a steel disk was fitted, designed to be coupled to a metal vane. At one of the extremities of this arm, different weights can be inserted, depending on the peak torque value desired. The brace positioned between the steel disk and the motor housing is at least 2 centimeters thick, and is appropriate to acquire torque in small spaces, and it can hold all of the electronic transduction.

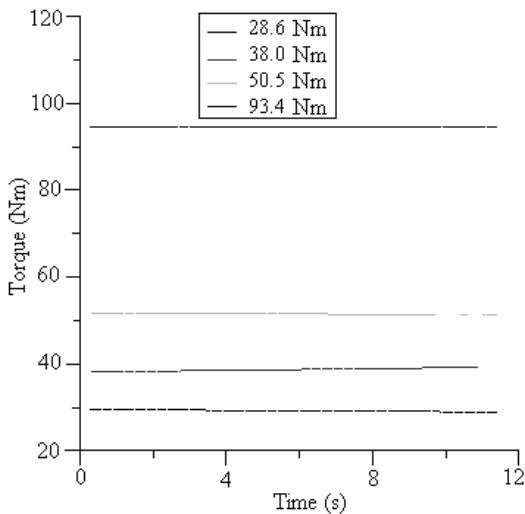


Figure 13. Curve regression in Fig. 12.



Figure 14. Dynamic torque II bench.

Figure 15 is a schematic of a rotating dynamic torque II bench. The torque meter can be calibrated varying the weights inserted at one of the extremities of the vane. For each weight inserted the motor is switched on and a sinusoid is obtained, whose peaks occur when the vane is in a horizontal position. Since the distance between the center of the vane and the center of the reference weights is known, the reference torque for calibration can be obtained by multiplying weight by distance, according to Eq. (7), see Fig. 16.

$$T_p = L \times P$$

$$T_p = 0.64 \times P \quad (7)$$

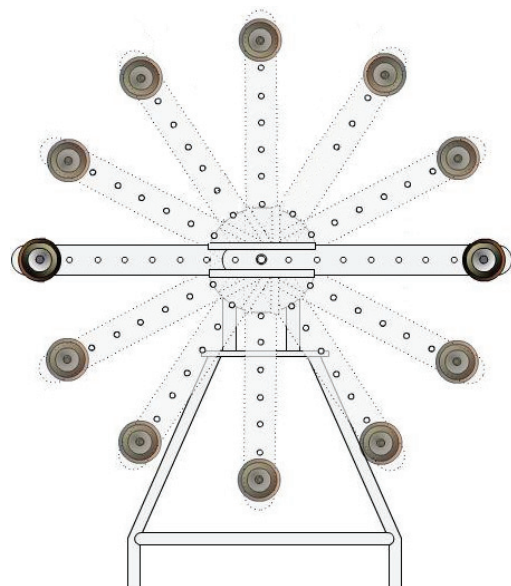


Figure 15. Rotating movement performed by the dynamic torque II bench.

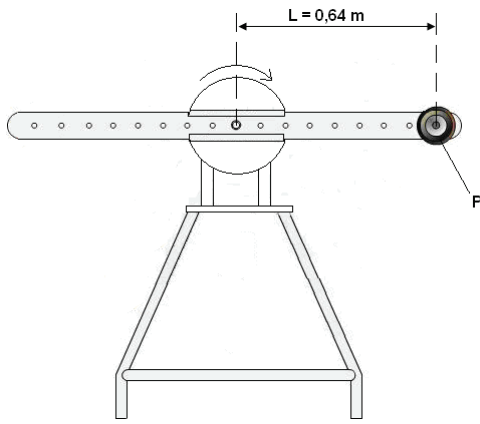


Figure 16. Illustration to calculate the reference torque.

Figure 17 shows an example of torque curve obtained using software in LabView.

The noise present in the sinusoid of Fig. 17, which is stronger in the downwards and upward direction close to the peaks, is justified by the vibration of the structure and by reducer decoupling. This was confirmed using a 12-bit AD converter which, through cables, obtained the curve of Fig. 18, where the same noisy phenomena are seen. The use of cables to perform this type of reading was only possible because of low reducer rotation, with the observation of a few cycles, the time required for the cables not to become coiled up that it would be impossible to perform an acquisition.

The calibration curve of the dynamic torque meter in Fig. 19 was obtained from the relationship between peak values of the voltage sinusoids shown by LabView, and the real torque obtained from Eq. (7).

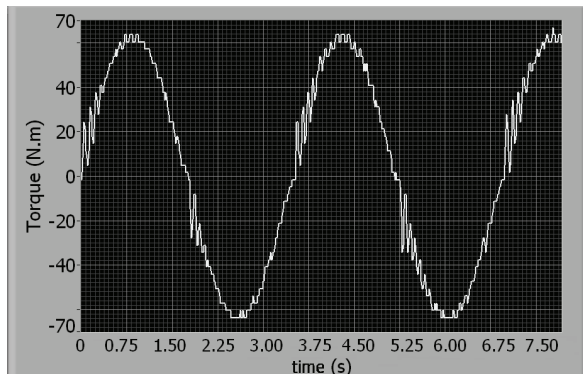


Figure 17. Torque curve obtained from simulation in the laboratory.

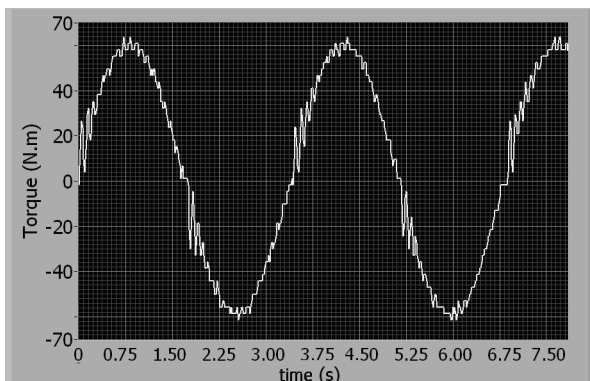


Figure 18. Torque curve with the same weight as Fig. 17, but obtained using cables with an AD converter.

Table 2, similarly to Table 1, relates the torque of the best-fit line of Fig. 19 and the torque calculated by method based on the value supplied by the strain gauge. The purpose of this table is to calculate the error caused by the method used in this study.

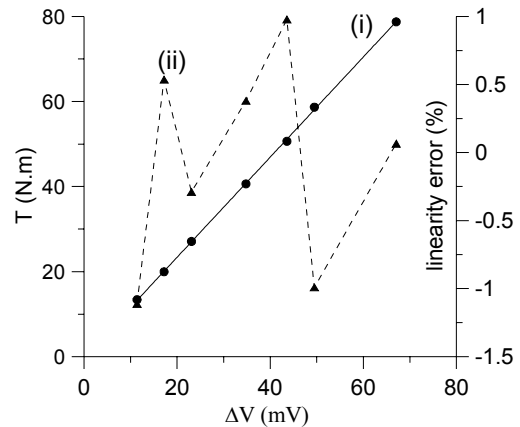


Figure 19. Experimental results: (i) Regression curve for dynamic torque calibration; (ii) the linearity error with respect to the best-fit line.

Table 2. Comparison between the reference values of the torque and the torque values resulting from the method used.

ΔV (mV)	Reference Torque (Nm)	Calculated Torque (Nm)	Relative error
11.38151	13.23707	12.61566	-4.69%
17.18151	20.06604	19.04458	-5.09%
23.08151	27.01276	25.58435	-5.29%
34.78151	40.78846	38.55304	-5.48%
43.58151	51.14967	48.30726	-5.56%
49.48151	58.09639	54.84703	-5.59%
67.06151	78.79526	74.33331	-5.66%

Analyzing the torque meter results in dynamic behavior, one reaches reach instrument uncertainty of 0.78% (linearity error) and a mean error of method of 5.34%.

A shaft of ABNT/SAE 1045 steel was used, with known properties that were applied in the torque calculation method, resulting in a mean error of 0.20%. In the case of the dynamic torque II bench, the reducer manufacturer does not say what material was used to make the shaft, and this led to using the same transverse elasticity constant of the static torque bench shaft to calculate torque. This may have contributed to the 5.34% deviation (mean error) despite a standard deviation of 0.35% of errors in the measures. Therefore, the properties of the material should be verified to correct the value used for calculation.

Another relevant issue is that, when measuring the dynamic torque, small torque values were read (maximum 78.7 Nm) compared to the instrument capacity (maximum 261.3 kN.m). This is due to the bench structure itself. The resolution of the A/D converter of ZigBee used is in the order of $3/1024 = 2.93$ mV, which is the equivalent of 3.45 N.m for the dynamic torque II bench. In other words, the resolution of the A/D converter impairs the precision of the system, since 3.45 N.m is the equivalent to 4.38% of the reading of maximum torque experienced.

Even with the bench vibration and the resolution problems of the ZigBee A/D converter belonging to the remote unit, there was

still an instrument uncertainty of 0.78%, which is reasonable for the state of the art dynamic torque meters, whose uncertainty fluctuates between 1% and 2% (Fujii, Ohgushi and Tojo, 1999).

Conclusions

This work is a theoretical and experimental study of a telemetric dynamic torque meter, which was an effective way to calculate dynamic torque, designed to eliminate a few limitations of conventional torque meters, without compromising acquisition quality. The use of wireless technology with digital modulation practically eliminates the noise caused by the coupling seen in other torque sensors, such as those that use slip rings or rotating transformers.

The brace allows real time monitoring of dynamic torque. It does not cause torsion error and protects the electronic circuits against environmental agents.

The ambient temperature variation is the main source of error in electronic transduction. Circuit assays are for a temperature variation of 50°C. Even for a temperature range well above the field work range, uncertainty only due to transduction electronics gave a result in the order of 0.05%. Therefore, the error in measuring is practically linked to the use of strain gages, which may be reduced by procedures and by the study of techniques appropriate to fix the strain gage on the shaft.

Using super batteries ensures autonomy of use for around several days, for continued use, and if an adequate procedure is maintained to install the components in the pumping unit, it is estimated that torque meter maintenance occurs at 24 month intervals.

A relevant factor is that the torque meter shown cost little compared to those available on the market. It is also relevant that most existing dynamic torque meters on the market have a limited range of action, due to the use of flanges and sockets to couple them to the shaft, while the instrument presented can be installed directly on the surface of a shaft. For this it is enough that the shaft be 1.5 cm wide to install the strain gage and couple the brace and flexible sealant.

The calibration of the instrument at the site where it is used, based on the dynamic torque, eliminates the deficiency of state of the art torque meters whose calibration is performed based in the static torque.

Since there has been no prior dynamic torque meter with such great coverage, and there is a growing need for adequate monitoring of the torque, it is hoped that this technology will be widely accepted in industry.

In coming studies, a transceiver module with a higher resolution ADC will be used and the intention is to eliminate the mechanical noise on the dynamic torque II bench, in order to find out the precise value of system uncertainty, which is estimated as less than 0.5%.

For future studies it is intended to double the number of strain gages used to increase sensitivity and annul the effect of ambient temperature on the reading of deformation.

It's already developed a low noise supply mechanism for the remote unit that eliminates the use of batteries and increases the system autonomy.

The signal is to become available in the industrial standard, immune to noise, from 4 to 20 mA to monitor torque in mechanical pumping oil extraction units. The signal received is to become available also in the MODBUS protocol.

Acknowledgements

The authors would like to thank *Conselho Nacional de Desenvolvimento Científico e Tecnológico* (CNPq) for financial support and PETROBRAS for the support received for this project on visits to their premises and for financial support.

References

- Antunes, J.M.V.C.D., 2003, "The Analysis Signed in the Quality Control Process (The Court of Ornamental Rocks)" (In Portuguese), Master's Dissertation, Technical University of Lisboa, Lisboa, Portugal, 76 p.
- Brito, R.M., 1994, "Sistema Eletro-Eletrônico para Medição Direta de Torque em Dispositivos Girantes Utilizando Extensômetros de Resistência Elétrica", Tese de Doutorado, Universidade Federal do Rio Grande do Sul, Porto Alegre, RS, Brasil, 145 p.
- Cheong, Y.D., Kim, J.W., Oh, S.H. and Lee, C.W., 1999, "Analysis and development of the angular twist type torque-meter", *Composite Structures*, Vol. 47, pp. 457-462.
- Dally, J.W., Riley, W.F. and McConnell, K.G., 1993, "Instrumentation for Engineering Measurements", Ed. John Wiley & Sons, 584 p.
- Doebelin, E.O., 1990, "Measurement Systems Application and Design", 4th edition, McGraw-Hill International Editions, New York, 960 p.
- Enciclopedia Britannica, 1986, Chicago, Vol. 5, 982 p.
- Filippin, C.G., Horbatiuk, B.W.D., Paula, A.C. et al., 2003, "Measurement of uncome groups in hydrogenerators" (In Portuguese), National Production and Transfer of Electrical Energy Seminar, GGH-12, Uberlândia, MG, Brasil, pp. 19-24.
- Fujii, Y., Ohgushi, K. and Tojo, T., 1999, "A proposal for a dynamic-response-evaluation method for torque transducers", *Measurement Science and Technology*, Vol. 10, pp. 142-144.
- Gerstenhaber M., Lee, S., 2004, "NA-683 Application Note – Strain Gage Measurement Using an AC Excitation", Analog Devices.
- Holman, J. P., 1984, "Experimental Methods for Engineers", 4th Edition, Ed. McGraw-Hill, Tokyo, 514 p.
- Kruger, L., Swart, P.L., Chtcherbakov, A.A. and Wyk, A.J., 2004, "Non-contact torsion sensor using fibre bragg gratings", *Measurement Science and Technology*, Vol. 15, pp. 1448-1452.
- Lima-Filho, A.C., 2007, "Telemetric Dynamic Torque Meter applied to the Reducer Shaft of an Oil Pumping Unit", Master's dissertation, Federal University of Paraíba, Joao Pessoa, PB, Brazil.
- Meng, Z. and Liu B., 2006, "Research on the laser doppler torque sensor", *Journal of Physics: Conference Series*, Vol. 48, pp. 202-206.
- Norton, H.N., 1969, "Handbook of Transducers for Electronic Measuring Systems", Ed. Prentice-Hall, 704 p.
- Olabi, A.G. and Grunwald, A., 2007, "Design and application of magnetostrictive materials", *Materials and Design*, doi:10.1016/j.matdes.2006.12.016.
- Preobrazhensky, V.P., 1980, "Measurements and Instrumentation in the Heat Engineering", Mir Publishers, URSS, 694 p.
- Sensotec, "Model 9300 Rotary Torque Measuring System", available on <http://www.sensotec.com/wdc/9300data.asp>, last visit: 18/01/2007.
- Tian X. and Tao X., 2000, "Torsion measurement by using FBG sensors", *Proceedings SPIE*, Vol. 4077, pp. 154-64.
- Wang, L.A., Lin, C.Y. and Chern G.W., 2001, "A torsion sensor made of a corrugated long period fibre grating", *Measurement Science and Technology*, Vol. 12, pp. 793-799.
- Wegener, G. and Andrae, J., 2006, "Measurement uncertainty of torque measurements with rotating torque transducers in power test stands", *Measurement*, Vol. 40, Issues 7/8, pp. 803-810.